

# Interannual variability of winter precipitation in Southeast China

Ling Zhang · Klaus Fraedrich · Xiuhua Zhu ·  
Frank Sielmann · Xiefei Zhi

Received: 9 September 2013 / Accepted: 26 January 2014 / Published online: 19 February 2014  
© Springer-Verlag Wien 2014

**Abstract** The observed winter (DJF) precipitation in Southeast China (1961–2010) is characterized by a monopole pattern of the 3-monthly Standardized Precipitation Index (SPI-3) whose interannual variability is related to the anomalies of East Asian Winter Monsoon (EAWM) systems. Dynamic composites and linear regression analysis indicate that the intensity of EAWM and Siberia High (SH), the position of East Asian Trough (EAT), and El Niño events and sea surface temperature (SST) anomalies over South China Sea (SCS) influence different regions of anomalous Southeast China winter precipitation on interannual scales. The circulation indices (EAWM index, SH index, and EAT index) mainly affect the winter precipitation in the eastern part of Southeast China. El Niño events affect the South China winter precipitation due to the anticyclone anomalies over Philippines. The effect of SCS SST anomalies on the winter precipitation is mainly in the southern part of Yangtze River. Thus, a set of circulation regimes, represented by a handful indices, provide the basis for modeling precipitation anomalies or extremes in future climate projections.

## 1 Introduction

Southeast China is located at the boundary of East Asian subtropical and tropical regions where weather and climate disasters bring frequent damage in winter. For example, in 2005 and 2008, extreme freezing rain and snow in Southern China resulted in considerable loss of life (Wen et al. 2009; Zhou et al. 2009a; Wu et al. 2011). Furthermore, numerous studies report that winter precipitation has increased significantly over South China in recent decades (Hu et al. 2003; Wang et al. 2004; Wang and Zhou 2005; Zhai et al. 2005; Su et al. 2006; Zhou and Yu 2006; Guo and Ding 2009; Zhi et al. 2010; Wang et al. 2012).

The atmospheric circulation patterns affecting South East China are influenced by continental and oceanic processes. One of the most influential components of the global climate system is the East Asian winter monsoon (EAWM) system. Climate variability in East Asia impacts both adjacent and distant regions (Zhang et al. 1997; Wang et al. 2000). In winter, the robust Siberian High (SH) appears over the Asian continent with a strong Aleutian Low to its east and a deepened East Asian trough in the lower troposphere (EAT, Chang et al. 2006; Wang et al. 2010). The most prominent surface feature of the EAWM is characterized by strong northwesterlies along the east flank of the SH and the East Asia Coast except for the South China Sea where northeasterlies prevail (Chen et al. 2000). An abnormal EAWM can induce circulation changes over East Asia (Chen et al. 2000; Chou et al. 2009; Zhou et al. 2011). Monsoon outbreak is accompanied by rapid southward intrusions of cold air bringing severe weather, such as gales, cooling, frost, rainstorms, freezing rain, and serious sandstorms, to most areas of East Asia (Ding 1994; Huang et al. 2003; Chang et al. 2006; Zhou et al. 2010; 2011).

The ocean as the largest underlying surface plays an important role in climate variability. Previous studies have

---

L. Zhang · K. Fraedrich · X. Zhi  
Collaborative Innovation Center on Forecast and Evaluation of  
Meteorological Disasters; KLME, Nanjing University of Information  
Science and Technology, Nanjing, China

L. Zhang (✉) · K. Fraedrich  
Max Planck Institute for Meteorology, Hamburg, Germany  
e-mail: zhang.ling@zmaw.de

X. Zhu  
KlimaCampus, Hamburg University, Hamburg, Germany

F. Sielmann  
Meteorological Institute, Hamburg University, Hamburg, Germany

shown that the tropical sea surface temperature (SST) has large influence on East Asia climate anomalies (Wang et al. 2000; 2002; Huang et al. 2003; Chou et al. 2009; Xie et al. 2009; Zhou et al. 2009b; 2010; Feng et al. 2011; Wang et al. 2012), which is also observed in winter (Zhang et al. 2002; Wu et al. 2003; Zhou et al. 2009a; 2010). For the South China precipitation, Zhou et al. (2010) indicate that ENSO and SST anomalies over South China Sea (SCS) independently influence precipitation anomalies in JFM (January–February–March), respectively. And Kim et al. (2013) studying the combined effect of ENSO and Pacific Decadal Oscillation (PDO) on the EAWM, shows that, when the ENSO and PDO are inphase, a negative relationship between ENSO and EAWM is significantly intensified.

In this paper, we focus on the interannual variability of Southeast China winter precipitation and aim to identify the relevant large-scale atmospheric and oceanic patterns and mechanisms. The paper is structured as follows: data and methods are described in Section 2; the interannual variability of Southeast China winter precipitation and associated atmospheric circulation are analyzed in Section 3; possible causes of Southeast China winter precipitation anomalies are presented in Section 4; the conclusion follows in Section 5.

## 2 Data, methods of analysis, and climatological setting

Monthly precipitation station observations in China are obtained from the National Meteorology Information Center, China Meteorological Administration, CMA. For the entire China 573 stations (1961–2010) are used by considering missing data; 232 stations available are analyzed for Southeastern China (marked in Fig. 1). Winter precipitation shows largest amplitudes of the climatological mean and, in particular, of the winter to winter variability in the Southeast of China (Fig. 1), because it is located at the boundary of East Asian subtropical and tropical regions. To assess drought and wetness the precipitation time series are transformed to Standardized Precipitation Indices (SPI, McKee et al. 1993; Bordi and Sutera 2001; Keyantash and Dracub 2002), because it is a suitable measure to compare regions or watersheds under different climate conditions, and to monitor drought/wetness by describing water deficit/surplus on meteorological, agricultural, and hydrological time scales ranging from months to years (Bordi et al. 2004; Bordi et al. 2009). In this study seasonal drought and wetness in winter is based on the 3-month (DJF) time scale (SPI-3) whose positive (negative) values indicate greater (less) than normal precipitation.

A subsequent empirical orthogonal function (EOF) analysis of the SPI-3 shows that temporal and spatial features of winter precipitation in Southeast China are suitably characterized by the dominating EOF with a uniform monopole as spatial pattern over South China (Fig. 2a); the corresponding

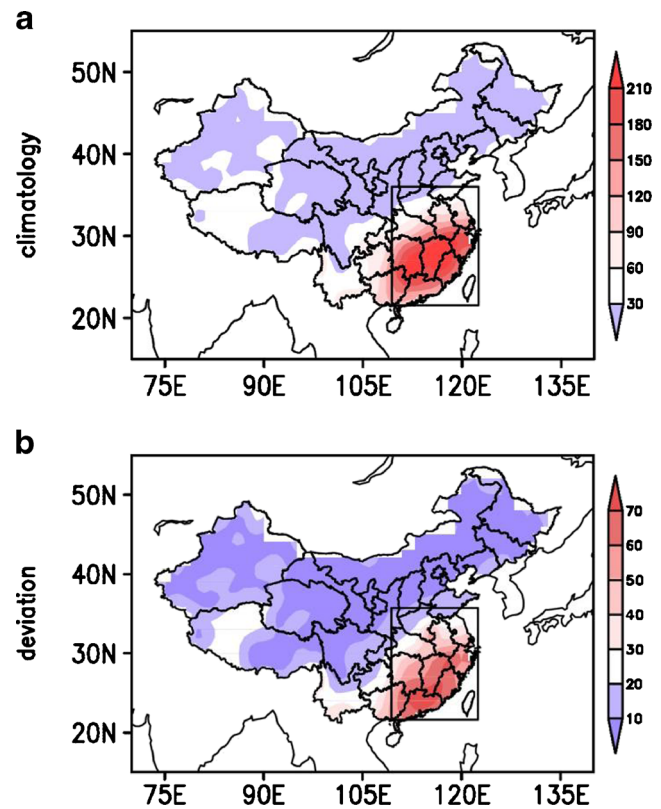


**Fig. 1** Winter (Dec.–Feb.) precipitation (mm/year) for 1962–2010: **a** mean and **b** standard deviation. *Rectangle* shows region of analysis (Southeast China)

time coefficient indicates both interannual and also interdecadal variability (Fig. 2b).

In order to highlight the year-to-year variability of winter precipitation in Southeast China, the interannual SPI-3 in Southeast China is obtained after removing the interdecadal signals (9-year running mean) from the original winter-to-winter SPI-3, which is subjected to the EOF analysis (Fig. 2c,d). The first EOF, which explains 37.2 % of the total variance, shows a pattern similar to first EOF of the original SPI-3 (Fig. 2a, c). The corresponding PC-1 characterizes the variability of the interannual winter precipitation of Southeast China and, therefore, defines a suitable index (IWPI: interannual winter precipitation index) to analyze the relation with large-scale circulation regimes. These are the East Asian Trough (EAT and its location), East Asian Winter Monsoon (EAWM and its intensity), Siberian High over the continent (SH and its intensity), and the sea surface temperature field near the equatorial Pacific (Niño 3.4) and the neighboring South China Sea (SCS in terms of area mean SST). These circulation regimes are characterized by the following indices: EAT index, EAWM index, SH index, Niño 3.4 index, and SCS index, which determine respective the intensities or location as quantitative measures the respective circulation regimes (see Table 1). All indices are normalized.

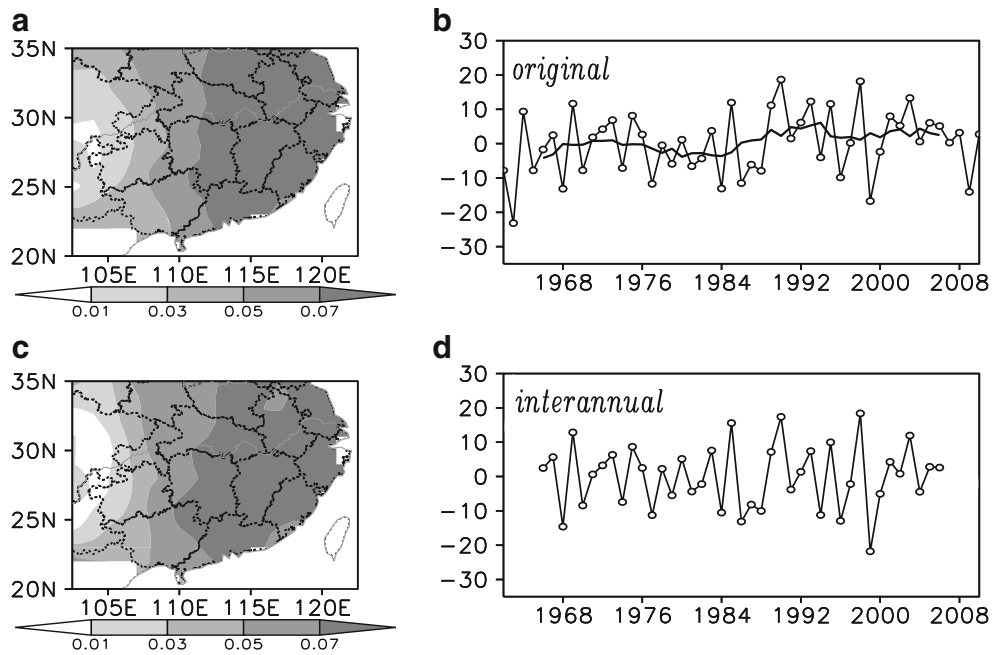


**Fig. 2** The 3-monthly Standardized Precipitation Index (SPI-3) and 9-year running mean of the winter mean in Southeast China: **a** first EOF, **b** time coefficients from original SPI-3 (*black smooth line* derived from 9-

year running mean); **c** first EOF, **d** time coefficients (IWPI: interannual winter precipitation index in Southeast China) from original minus 9-year running mean

### 3 Interannual variations of precipitation and associated circulation influences

In the following, we employ composite analysis to examine associated circulation anomalies of anomalous precipitation in Southeast China on interannual time scales. Anomalous positive (negative) years are defined when the standardized IWPI is greater (less) than 1(−1), equivalent to ±1 standard deviation of IWPI. Thereby we get wet than normal years comprising 1975, 1983, 1985, 1990, 1995, 1998, 2003, and dry than normal years including 1968, 1974, 1977, 1979, 1984, 1986, 1988, 1994, 1996, and 1999.

The geopotential height anomalies at 500 hPa indicate that, when the precipitation is more intense than normal, anomalous positive geopotential heights extend from Northeast China to the North Pacific Ocean and most of the Eurasia continent is

controlled by anomalous negative geopotential heights (Fig. 3a). That is, the East Asian Trough and the Baikal ridge are weakened and the associated meridional circulation is weaker than normal over mid- to high latitudes. Thus, cold air from the north is not supported to move southward. Over mid- to low latitudes, when precipitation is stronger, significant anomalous negative geopotential heights appear over the Bay of Bengal, strengthening the Bay of Bengal Trough and thus enhancing the meridional circulation. Thus warm and humid air from the Indian Ocean is transported to the South China and moisture transport over SCS is strengthened (see Fig. 3b for 850 hPa moisture transport anomalies). Two major transport channels are observed: one extends from the North Indian Ocean through India and the Bay of Bengal to Southwest China, and the other from the South Pacific Ocean through the maritime continents and the SCS towards South China. These two anomalous moisture flux

**Table 1** The definition of indices

Pattern	Definition	Index
El Niño events (Niño 3.4)	SST area mean (5° N–5° S, 120°–170° W)	Niño 3.4>0: El Niño Niño 3.4<0: La Niño
South China Sea SST (SCS)	SST area mean (10°–20° N, 110°–120° E)	SCS>0: warm SCS<0: cold
East Asian Winter Monsoon (EAWM)	Zonal SLP differences (110° E minus 160° E, sum from 20° N to 70° N)	EAWM>0: strong EAWM<0: weak
East Asian Trough (EAT)	Longitude (100°–160° E) of min 500 hPa geop. height (N-Hemisphere mean)	EAT>0: eastward EAT<0: westward
Siberian High (SH)	SLP area mean (20°–70° N, 80°–120° E)	SH>0: strong SH<0: weak

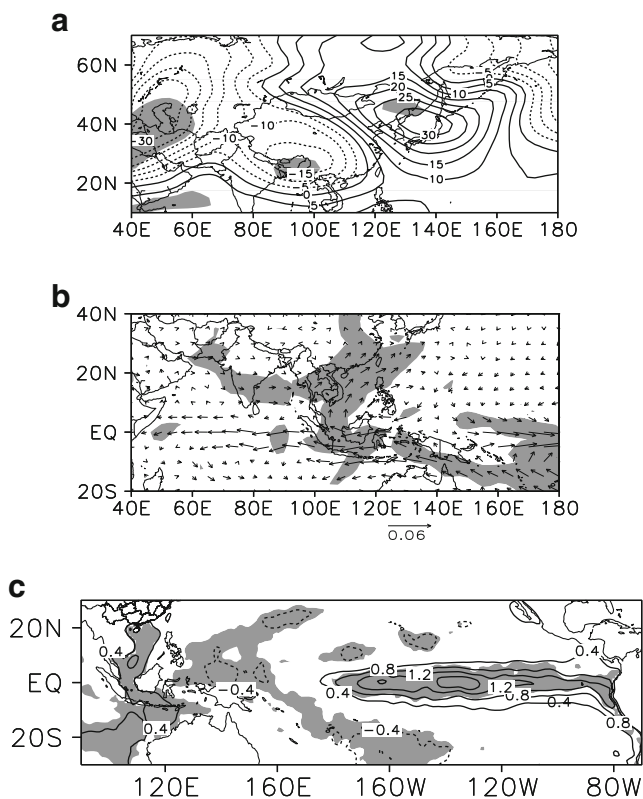


**Fig. 3** Composites of geopotential height in gpm (a), moisture flux at 850 hPa in (m-g)/(kg-s) (b), and sea surface temperature in °C (c) differences of positive minus negative anomalous years of the IWPI and shaded areas are statistically significant at 90 % confidence level

channels transport warm moist air northward from tropical oceans and thus contribute to positive specific humidity anomalies in the coastal areas of Southeast China (Fig. 3b), where warm air from the south combined with cold air from the north provide favorable conditions for precipitation formation.

#### 4 Possible causes of Southeast China winter precipitation

Northwestward moisture fluxes along coastal areas in Southeast China (Fig. 3b) suggest a weaker EAWM. We have analyzed the composite heating differences between ocean and land, without visible changes being detected (not shown) in the mid- and high latitudes. But the temperature fields show remarkable anomalies in lower latitudes, suggesting that they are mainly influenced by weather/climate systems from the south. Therefore, in the following section the impact factors affecting mid- to high latitudes and mid- to low latitudes are analyzed as possible causes of anomalous Southeast China winter precipitation.

##### 4.1 Anomalous mid- and high latitude circulation

According to the analysis of Section 3, wet winter years of Southeast China are characterized by a weak EAT and the

Baikal ridge (towards the west) associated with a weaker than normal meridional circulation over mid- to high latitudes. As the meridional (northerly) wind anomaly is the main characteristics of EAWM, its relation with the EAT, EAWM, and Siberia High (high correlated with EAWM) are discussed in this section.

The EAWM is described by an intensity index, determined by zonal Sea Level Pressure (SLP) differences ( $110^{\circ}$  E minus  $160^{\circ}$  E of the sum from  $20^{\circ}$  N to  $70^{\circ}$  N, see Shi et al. 1996; Wu et al. 2003). Based on the definition of Wu et al. (2003), an intensity index SH for the Siberian High is defined as regionally averaged SLP ( $20^{\circ}$  N– $70^{\circ}$  N,  $80^{\circ}$  E– $120^{\circ}$  E). And the EAT position index is determined by longitude ( $100^{\circ}$ – $160^{\circ}$  E) of minimum 500 hPa geopotential height (N-Hemisphere mean). The interannual time series of each index is obtained after removing the 9-year running mean from the original winter-to-winter indices. On interannual time scales EAWM index and EAT index are significantly correlated ( $-0.47$  and  $0.36$ , respectively) with the precipitation anomalies over Southeast China. The SH intensity is relatively highly related to precipitation in Southeast China, but its statistical significance does not pass 90 % confidence level (for other correlations see Table 2 and Fig. 7).

The correlation analysis is supplemented by a composite analysis of the winter precipitation over Southeast China employing a resampling test (Fig. 4). From the period 1962–2010, the five lowest and five highest values of each of the indices are selected and the anomalous years of each index are shown in the Table 3. Then the 5 years averages of SPI-3 in the low index ( $P_L$ ) and high index ( $P_H$ ) years are computed, respectively. The ( $P_H - P_L$ ) differences between the years with lowest and highest precipitation give an indication of the influence of the possible impact factors (EAT, EAWM, and SH) affecting each station. A resampling method (Zhang et al. 2010), which determines whether the differences are significant, is performed as follows: First, a station averaged SPI-3 from two randomly selected 5-year samples provide the difference (dPmax) in the averages for the two 5-year samples. Then this process is repeated 1,000 times and, finally, ranked from large to small order. The association between possible causes and winter precipitation over Southeast China is determined to be statistically significant at the 10 % level, if  $P_H - P_L$  greater than the 100th largest dPmax value (shaded regions in Fig. 4).

**Table 2** The correlation coefficients between different indices

	SCS	EAWM	EAT	SH	IWPI
Niño 3.4	0.41 <sup>a</sup>	-0.28 <sup>a</sup>	-0.28 <sup>a</sup>	-0.18	0.34 <sup>a</sup>
SCS		-0.61 <sup>a</sup>	-0.01	-0.34 <sup>a</sup>	0.27 <sup>a</sup>
EAWM			-0.05	0.75 <sup>a</sup>	-0.47 <sup>a</sup>
EAT				-0.32 <sup>a</sup>	0.36 <sup>a</sup>
SH					-0.24

<sup>a</sup> Significant > 0.1 level ( $\pm 0.264$ )

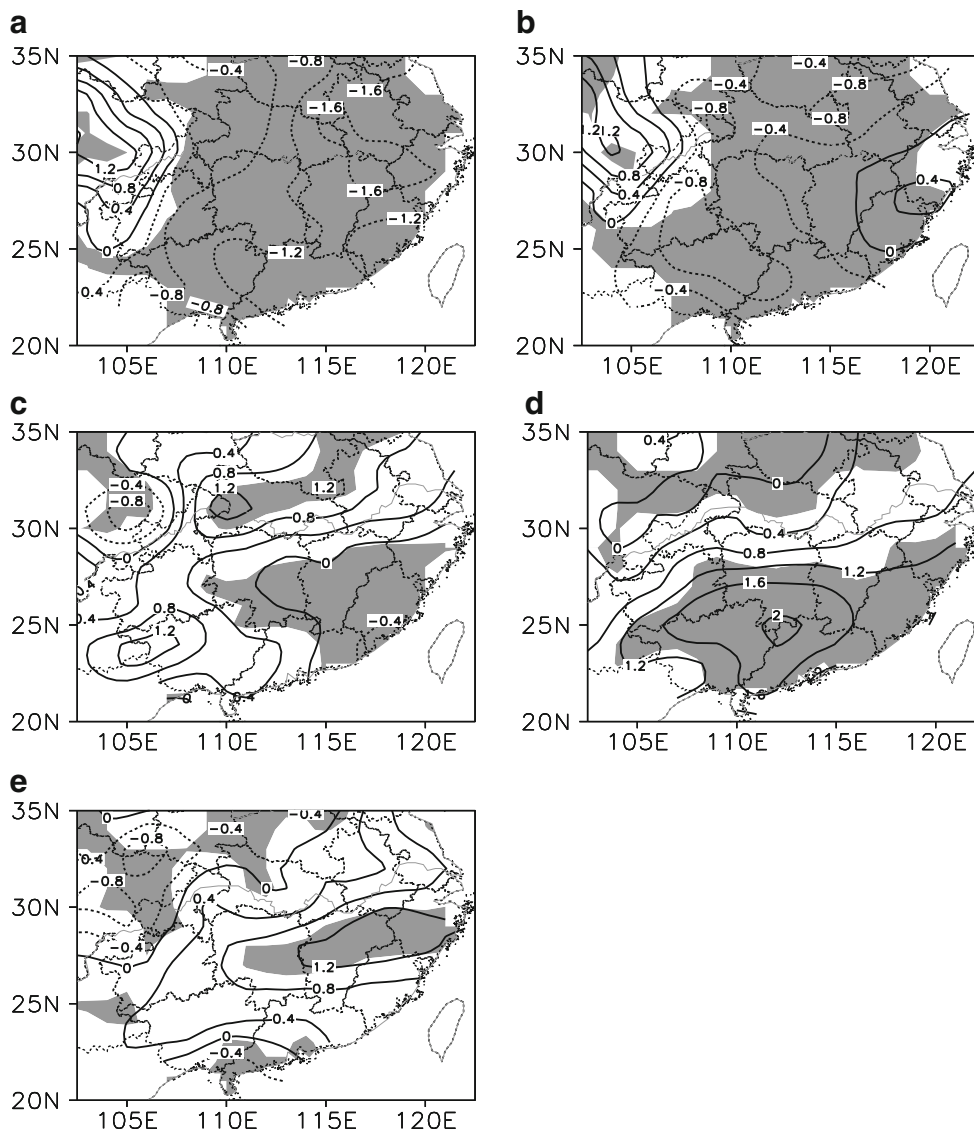


**Fig. 4** Composites of SPI-3 differences of positive minus negative anomalous years of each index and shaded areas are statistically significant at 90 % confidence level: **a** East Asian winter monsoon; **b** Siberia High; **c** East Asian Trough; **d** El Niño; **e** sea surface temperature anomalies of South China Sea

The composite analysis of SPI-3 over Southeast China (Fig. 4) reveals that each index is related to its specific significant winter precipitation anomaly over Southeast China: (1) EAWM (Fig. 4a) mainly influences the anomalous precipitation

over east part of Southeast China, which is similar to the results of SH (Fig. 4b), but EAWM has larger effect on the precipitation anomalies. (2) EAT enhances winter wetness or dryness over the northeastern part of Southeast China (Fig. 4c).

**Table 3** Anomalous years of each index on interannual time scales

Niño 3.4		SCS		EAWM		SH		EAT	
Strong	Weak	Strong	Weak	Strong	weak	Strong	Weak	East	West
1973	1971	1966	1968	1968	1969	1977	1973	1973	1972
1983	1974	1963	1976	1977	1972	1984	1979	1987	1986
1992	1976	1988	1984	1984	1973	1996	1987	1993	1994
1995	1989	1998	1996	1986	1979	2000	1997	2001	2005
1998	2000	1999	2004	1996	1990	2005	2004	2004	2006

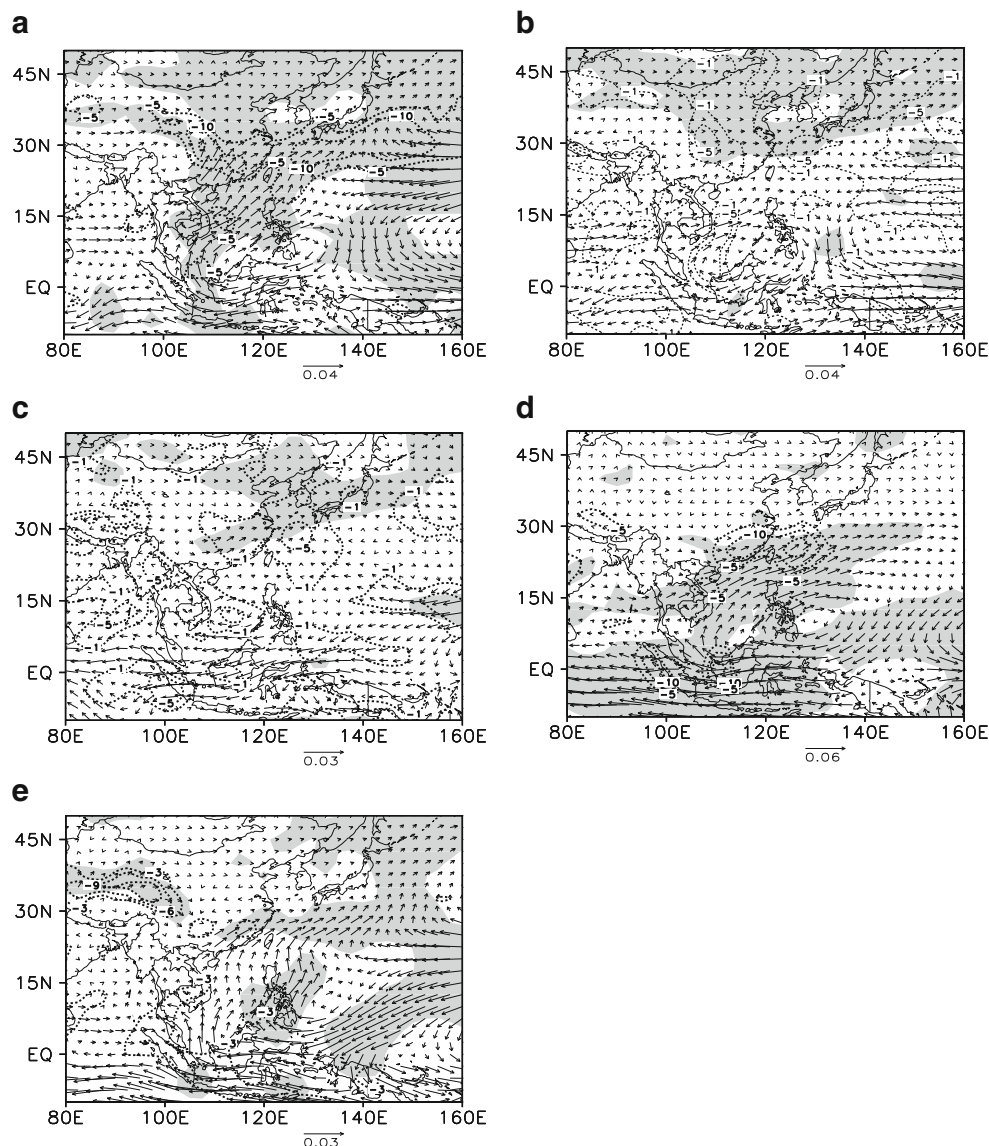


**Fig. 5** Composites of moisture flux (vectors;  $(\text{m}\cdot\text{g})/(\text{kg}\cdot\text{s})$ ) and divergences (dotted lines  $10^{-5} \text{ g}/(\text{kg}\cdot\text{s})$ ) differences of anomalous years with different indices at 850 hPa and shaded areas are statistically significant at 90 % confidence level: **a** East Asian winter monsoon (negative minus

positive); **b** Siberia High (negative minus positive); **c** East Asian Trough (positive minus negative); **d** El Niño (positive minus negative); **e** SST anomalies of SCS (positive minus negative)

The moisture flux anomalies at 850 hPa (Fig. 5) indicate that, when EAWM (Fig. 5a) is weaker than normal, an anticyclone appears over the Philippines which transports moisture along its northwestern part towards South China across the SCS. On the other hand, anomalous moisture flux by the mid-latitude westerlies affects the North and Northeast China. These two water transport channels provide positive moisture anomalies observed in the eastern part of China during weak EAWM years, which is a favorable situation for supplying abundant water vapor to South China and subsequently feeding the precipitation increase over there. During the years of a weaker SH (Fig. 5b), the geographical distributions of moisture flux anomalies are similar to those with weaker EAWM anomalies, but the significant regions range from the north of Yangtze River Valley to

Northeast China. For the EAT anomalous years (Fig. 5c), the anomalous moisture flux cannot be observed in lower latitudes while the significant positive moisture flux anomalies occur over middle to lower reaches of Yangtze River basin but with much lower magnitude. When EAT is located further eastward, the northerly flow is weaker than normal over the east coast of China (not shown, the position of EAT has positive relationship with meridional wind) which, due to enhanced eastward and northward water vapor transport towards the mid- and higher latitudes of eastern China, generates positive precipitation anomalies in the north part of Yangtze River basin.

In summarizing, correlation and composite analyses show that EAWM, SH, and EAT influence the winter precipitation in

the target region of Southeast China significantly. Correlations of 0.87 (or  $-0.32$ ) are observed between SH intensity index and EAWM intensity index (or EAT position index). That is, a weaker SH is associated with a more eastward (westward) EAT location leading to a weaker (stronger) EAWM due to weaker (stronger) northerlies along China's east coast. These circulation anomalies lead to intense (weak) northward moisture transports and thus to positive (negative) anomalous precipitation in Southeast China.

#### 4.2 Sea surface temperature influences

The composite analysis of sea surface temperature shows that (Fig. 3c), when the precipitation is more intense than normal, anomalous positive SST appears in the SCS and equatorial central and eastern Pacific Ocean and negative SST occurs in the western Pacific Ocean. This anomalous SST pattern over Pacific Ocean is similar to the El Niño SST field. That is, El Niño events and SST anomalies over SCS are closely related with Southeast China precipitation anomalies. In this study, Niño 3.4 index is used to describe El Niño events and SCS SST averaged over the region of  $10^{\circ}$ – $20^{\circ}$  N,  $110^{\circ}$ – $120^{\circ}$  E is taken as SCS index. The correlation coefficients of Southeast winter precipitation are 0.34 with Niño 3.4 index and 0.27 with SCS index, which shows ENSO and SCS SST anomalies playing a prominent role affecting Southeast China winter precipitation.

The composite analysis of SPI-3 over Southeast China (subjected to a resampling test, Fig. 4) reveals that El Niño events mainly affect winter precipitation anomalies over South China (Fig. 4d). Significant winter precipitation anomalies, which are influenced by SCS SST anomalies, occur over the south part of Yangtze River (Fig. 4e).

For El Niño years, previous studies (Wang et al. 2000; Zhou et al. 2009a; 2011; Feng et al. 2011) have shown an anomalous anticyclone observed over the Philippines and anomalous cyclonic circulation over the equatorial central and eastern Pacific. These circulation anomalies are consistent with the pattern shown in Fig. 5d. The anomalous anticyclone over the Philippines with southwesterly prevailing over South China enhance a warm and moist air transport to South China from South Pacific across SCS favoring precipitation formation in South China. Another transport channel is observed which supplies water vapor from the Indian Ocean through Bay of Bengal to Southeast China along northwestern part of the anomalous anticyclone over the Philippines. Thus, El Niño, which is closely associated with the anticyclone over Philippines, supports warm moist air transport northeastward; reducing the intensity of northerlies over Southeast coast of China indicates EAWM being weaker than normal. Note that the abundant moisture transport associated with El Niño is not comparable with the anomalous EAWM cases, with moisture transports from SCS across South China mainland to East China Sea with southwesterly flow instead of northerlies

extending to the mainland. These air circulation anomalies are favorable for enhancing precipitation over South China (Fig. 4d). When anomalous positive SST appears in SCS, the anomalous warm moist air moves further north compared to the El Niño cases (Fig. 5e). And the moisture flux converges over south part of Yangtze River with anomalous ascending motions, which is favorable for enhancing the precipitation over south part of Yangtze River basin (Fig. 4e). Despite the strong correlation between Niño 3.4 index and SCS index (with a significantly positive index correlation of 0.43), it is possible to separately analyze the effect of one (of the two) signals, El Niño or SCS SST anomalies, once the other's linear regression field is separated from the original. For the El Niño years without SCS SST anomalies influences, the anomalous moisture flux transports to South China along northwestern part of anomalous Philippines anticyclone and results in the precipitation increasing over South China. So, the effect of El Niño and SCS SST anomalies on the Southeast China winter precipitation is relative independent on interannual scales. Similar results (not shown) emerge for positive SCS SST anomalies without ENSO effects. Abundant water vapor is transported to the Southeast China accompanied by southwesterlies and southwesterlies converging over the southern part of Yangtze River basin where the precipitation enhances.

#### 4.3 Linear regression analysis

According to the above discussions, EAWM, SH, EAT, El Niño, and SST anomalies of SCS affect the Southeast China winter precipitation anomalies significantly in different regions of Southeast China. Linear regression is used to prove the effect of each individual impact factor. Employing  $R^2$  statistics, the explained variances,  $R^2=1-SSE/SST$ , quantify how successful a linear model replicates the station observations; here SSE (SST) is the mean squared error (variance).

The geographical distributions of the  $R^2$  measure associated with different indices are shown in Fig. 6. The patterns of variances explained by the linear regression are similar compared to the SPI-3 composites (Fig. 4). For Niño 3.4 index, the relative high values of explained variances are located in the South China with maximum over about 20 %. Index characterizing the SST anomalies over SCS fits SPI-3 over the southern part of Yangtze River with higher explained variances; the EAWM intensity index shows high-value regions of explained variances at the east coast of China; the SH intensity and EAT position indices reveal relative high values of explained variance in the northeastern part of Southeast China. Thus, each individual index explains high magnitudes of the SPI-3 variations in different regions of Southeast China. Due to the close relationship between the indices and SPI-3 over Southeast China, multi-linear regression is applied to fit the SPI-3 over Southeast China (Fig. 6f). Multi-linear regression of the five indices (EAWM index, SH index, EAT index, Niño

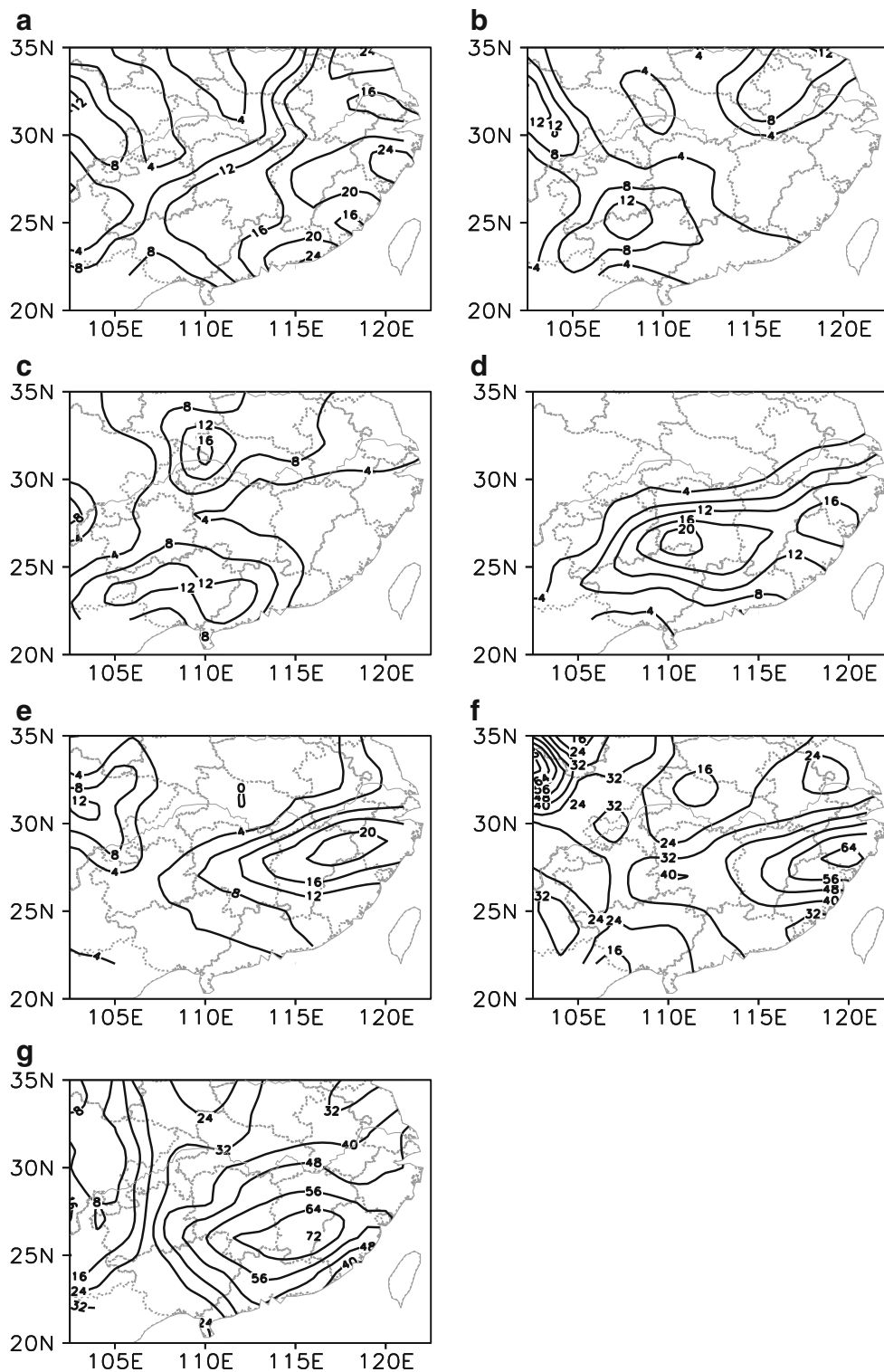


**Fig. 6** Geographical distribution of the  $R^2$  statistics (units: %; the explained variances) for linear regression with different indices: **a** East Asian winter monsoon; **b** Siberia High; **c** East Asian Trough; **d** El Niño; **e** SST anomalies of SCS; **f** multi-regression with five indices; **g** IWPI

3.4 index, and SCS index) with station SPI-3 show high values of explained variances over most parts of Southeast China with maximum values exceeding 60%; regression with the EOF-based index IWPI (Section 2) shows similar results

(Fig. 6g). In summarizing, all five impact factors, EAWM, SH, EAT, El Niño, and SST anomalies over SCS, play important roles in the interannual variability of winter precipitation in Southeast China, especially in the eastern part.

## 5 Summary and conclusion

Winter precipitation variability of Southeast China on interannual time scales involves the intensities of the East Asian Winter Monsoon and Siberian High, the position of the East Asian Trough and the sea surface temperature and their associated moisture flows in the lower troposphere (Fig. 7). Using the standardized precipitation index (SPI) to monitor winter wetness and dryness in Southeast China (SPI of 3 months) interannual variability is captured by subtracting 9-year running mean from the original data. The first EOF of the interannual components of SPI-3 describes 37.2 % of the space-time variability. The associated principal components serve as indices to characterize wetness–drought variability and its relation with the large-scale atmospheric circulation patterns governing the winter climate of East Asia. The following results are obtained:

- (i) On interannual scales, the dominating spatial pattern of wetness and drought intensity is uniform in Southeast China. During wet (dry) winter of Southeast China the northward warm moist air over East China from Indian Ocean and South Pacific is strengthened (weakened). And the associated circulation indicates the Bay of Bengal Trough (BBT) to be stronger (weaker) than normal over the low to mid-latitudes while the East Asian Trough and the Baikal Ridge are weaker (stronger) than normal over mid- to high latitudes in wet (dry) winters.
- (ii) Over mid- to high latitudes, the composite analysis with resampling test indicates that EAWM plays an important role for the interannual variability of Southeast China winter precipitation. The wet (dry) winter is a result of the enhanced (reduced) northward flow of warm and moist air over east coast of China caused by a weakened (strengthened) EAWM due to weakening (strengthening) of SH and eastward (westward) extension of EAT.

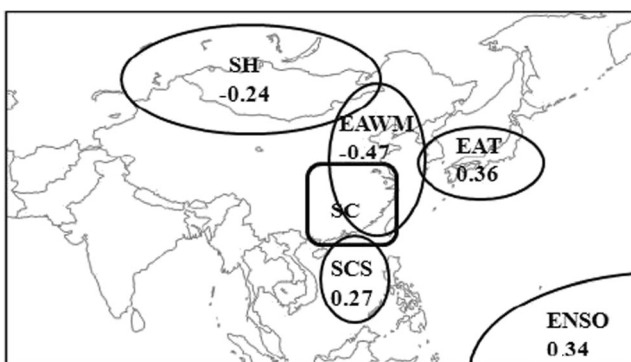


**Fig. 7** Location of atmospheric and oceanic patterns: East Asian winter monsoon (EAWM), Siberia High (SH), East Asian Trough (EAT), El Niño (ENSO), SST anomalies of SCS (SCS), and Southeast China (SC). And their contributions to the target region Southeast China precipitation in terms of correlation with the interannual winter precipitation index

- (iii) Over mid- to low latitudes, the circulation anomalies associated with Southeast China winter precipitation are closely related to El Niño events and sea surface temperature anomalies over the South China Sea. El Niño events affect the South China winter rainfall due to the anti-cyclonic flow anomalies over the Philippines. The effect of SCS SST anomalies on the winter precipitation occurs mainly in the southern part of the Yangtze River basin. Both composite and linear regression analyses reveal that the influences of SCS SST anomalies and El Niño events on the interannual variability of Southeast precipitation are different and independent.
- (iv) Based on linear and multi-linear regression analyses, the high variances of winter precipitation explained by the anomalous indices associated with EAWM, SH, EAT, El Niño, and SCS SST occur in different regions of Southeast China. All the indices give contributions to the interannual variability of Southeast winter rainfall, especially in the eastern part (Fig. 6).

The methods of analysis applied here and the results obtained provide a first step to assess a pronounced regional precipitation pattern in Eastern Asia; its mean and variability are dominated by a complex setting of flow regimes, whose intensities can be suitably characterized by circulation indices. In this sense methods and results form a basis to validate Regional and Global Climate Model simulations and to analyze changing precipitation fields of future scenarios in terms of changing circulation statistics.

**Acknowledgment** This study acknowledges the support of the National Basic Research Program “973” of China (2012CB955200), Key Laboratory of Meteorology Disaster of Ministry of Education (KLME1102), Max Planck of Meteorology Institute (MPI) fellowship, and Priority Academic Program Development of Jiangsu Higher Education Institutions (PAPD).

## References

- Bordi I, Sutera A (2001) Fifty years of precipitation: some spatially remote teleconnections. *Water Resour Manag* 15:247–280
- Bordi I, Fraedrich K, Jiang JM, Sutera A (2004) Spatio-temporal variability of dry and wet periods in eastern China. *Theor Appl Climatol* 79:81–91
- Bordi I, Fraedrich K, Sutera A (2009) Observed drought and wetness trends in Europe: an update. *Hydrol Earth Syst Sci* 13:1519–1530
- Chang CP, Wang Z, Hendon H (2006) The Asian winter monsoon. *The Asian Monsoon*, Wang B, Ed., Praxis, Berlin, 89–127.
- Chen W, Graf HF, Huang RH (2000) The interannual variability of East Asian winter monsoon and its relation to the summer monsoon. *Adv Atmos Sci* 17:48–60

- Chou C, Huang LF, Tu JY, Tseng L, Hsueh YC (2009) El Niño impacts on precipitation in the western North Pacific-East Asian sector. *J Clim* 22:2039–2057
- Ding YH (1994) Monsoon over China. Kluwer Academic Publishers: 420pp
- Feng J, Li J (2011) Influence of El Niño Modoki on spring precipitation over south China. *J Geophys Res* 116, D13102. doi:10.1029/2010JD015160
- Guo YJ, Ding YH (2009) Long-term free-atmosphere temperature trends in China derived from homogenized in situ radiosonde temperature series. *J Clim* 22:1037–1051
- Hu ZZ, Yang S, Wu R (2003) Long-term climate variations in China and global warming signals. *J Geophys Res* 108(D19):4614. doi:10.1029/2003JD003651
- Huang RH, Zhou LT, Chen W (2003) The progresses of recent studies on the variabilities of the East Asian monsoon and their causes. *Adv Atmos Sci* 20:55–69
- Keyantash J, Dracup JA (2002) The quantification of drought: an evaluation of drought indices. *Bull Am Meteorol Soc* 83:1167–1180
- Kim ST, Cai WJ, JIN FF, Yu JY (2013) ENSO stability in coupled climate models and its association with mean state. *Clim Dyn*. doi:10.1007/s00382-013-1833-6
- McKee TB, Doesken NJ, Kleist J (1993) The relationship of drought frequency and duration to time scales. Proc. Of the 8th conference on applied climatology, 17–22 January, Anaheim, CA, American Meteorological Society, Boston, MA, 179–184.
- Shi N, Lu J, Zhu Q (1996) East Asian winter/summer monsoon intensity indices with their climatic change in 1873–1989. *J Nanjing Inst Meteorol* 19(2):168–176 (in Chinese)
- Su BD, Jiang T, Jin WB (2006) Recent trends in observed temperature and precipitation extremes in the Yangtze River basin, China. *Theor Appl Climatol* 83:139–151
- Wang L, Chen W (2010) How well do existing indices measure the strength of the East Asian winter monsoon? *Adv Atmos Sci* 27:855–870
- Wang B, Zhang Q (2002) Pacific-East Asian Teleconnection. PartII: how the Philippine Sea Anomalous Anticyclone is established during El Nino development. *J Clim* 15:3252–3265
- Wang Y, Zhou L (2005) Observed trends in extreme precipitation events in China during 1961–2001 and the associated changes in large-scale circulation. *Geophys Res Lett* 32, L09707. doi:10.1029/2005GL022574
- Wang B, Wu RG, Fu XH (2000) Pacific-East Asian Teleconnection: how does ENSO affect East Asian climate? *J Clim* 13:1517–1536
- Wang S, Zhu J, Cai J (2004) Interdecadal variability of temperature and precipitation in China since 1880. *Adv Atmos Sci* 21:307–313
- Wang X, Wang DX, Zhou W, Li CY (2012) Interdecadal modulation of the influence of La Niña events on mei-yu precipitation over the Yangtze River valley. *Adv Atmos Sci* 29(1):157–168
- Wen M, Yang S, Kumar A, Zhang P (2009) An analysis of the large-scale climate anomalies associated with the snowstorms affecting China in January 2008. *Mon Weather Rev* 137:1111–1131
- Wu R, Hu ZZ, Kirtman BP (2003) Evolution of ENSO-related precipitation anomalies in East Asia and the processes. *J Clim* 16:3741–3757
- Wu Z, Li J, Jiang Z, He J (2011) Predictable climate dynamics of abnormal East Asian winter monsoon: once-in-a-century snowstorms in 2007/2008 winter. *Clim Dyn* 37:1661–1669
- Xie SP, Hu K, Hafner J (2009) Indian Ocean capacitor effect on Indo-Western Pacific climate during the summer following El Niño. *J Clim* 22:730–747
- Zhai PM, Zhang XB, Wan H, Pan XH (2005) Trends in total precipitation and frequency of daily precipitation extremes over China. *J Clim* 18:1096–1108
- Zhang RH, Sumi A (2002) Moisture circulation over East Asia during El Niño episode in Northern winter, spring and autumn. *J Meteorol Soc Japan* 80:213–227
- Zhang XB, Wang JF, Zwiers FW, Groisman PY (2010) The influence of large-scale climate variability on winter maximum daily precipitation over North America. *J Clim* 23:2902–2915
- Zhang Y, Wallace JM, Battisti DS (1997) ENSO-like interdecadal variability: 1900–1993. *J Clim* 10:1004–1020
- Zhi XF, Zhang L, Pan JL (2010) An analysis of the winter extreme precipitation events on the background of climate warming in Southern China. *J Trop Meteorol* 16(4):325–332
- Zhou LT (2011) Impact of East Asian winter monsoon on precipitation over southeastern China and its dynamical process. *Int J Climatol* 31:677–686
- Zhou LT, Wu RG (2010) Respective impacts of the East Asian winter monsoon and ENSO on winter precipitation in China. *J Geophys Res* 115, D02107. doi:10.1029/2009JD012502
- Zhou TJ, Yu RC (2006) Twentieth-century surface air temperature over China and the globe simulated by coupled climate models. *J Clim* 19:5843–5858
- Zhou LT, Tam CY, Zhou W, Chan JCL (2009a) Influence of South China Sea SST and the ENSO on winter precipitation over South China. *Adv Atmos Sci*. doi:10.1007/s00376-009-9102-7
- Zhou W, Chan JCL, Chen W et al (2009b) Synoptical-scale controls of persistent low temperature and icy weather over southern China in January 2008. *Mon Weather Rev* 137:3978–3991